Regional identification, partition, and integral phase unwrapping method for processing moiré interferometry images

Wei Qiu, Yi-Lan Kang, Qing-Hua Qin, and Wei-Tang Li

We present a new method of regional identification, partition, and integral (RIPI) phase unwrapping for processing images, especially those with low quality, obtained from moiré interferometry experiments. By introducing the principle of preorder traversal of a general tree in data structures and then by applying the idea of a regional integral, the proposed method makes regional partition and phase evaluation much easier and more accurate, and it also overcomes the common faults that can occur when conventional approaches, such as line defects, are used. Examples are given to demonstrate the advantage and applicability of the proposed RIPI method when processing experimental images. It is shown that the proposed method works well for global phase distribution, and, at the same time, local mutational information is preserved and limited to its vicinity without affecting other parts.

OCIS codes: 100.5070, 120.3180, 120.4120.

1. Introduction

Moiré interferometry is an optical experimental technique that is used to detect planar deformation of specimens by use of coherent laser light.[1] Owing to its advantages of high sensitivity, excellent contrast, noncontact, real time, and whole field measurement, moiré interferometry has been widely applied to deformation measurements in material science as well as mechanical and electronic engineering.[1–3] Previous studies of the applications[2,3] of moiré interferometry to deformation analysis of smart materials and structures at microscale and with multifield coupling brought forward some new requirements or issues for subsequent image processing such as phase unwrapping.[4,5] It is difficult to handle the issues detailed below with the existing methods.[6] First, the deformation of a specimen always appears small in comparison with the dimension of the specimen, but it is significant in the sense of a local dimension. Second, images obtained from experiments with multifield coupling are usually of low quality with numerous asymmetrical noises. Furthermore, defects in the gratings of microscale specimens are almost unavoidable during specimen preparing. Therefore, not only the locally acute deformation but also the noises and the grating defects can act as local phase dissimilarities and mutations in wrapped images, which make the corresponding image processing more difficult. Ideally, the locally acute deformation should not be neglected or averaged, and the noises and the grating defects should not be spread or propagated. However, it is difficult to distinguish them by use of traditional unwrapping methods.

Investigation of unwrapping algorithms have progressed,[7] such that they can be classified into four major categories[8]: local (path-following) integral,[4,9–17] global integral,[18–22] regional,[22–26] and temporal.[27,28]

The local (path-following) integral method integrates wrapped phases pixel by pixel along certain sequential paths[4,9,10,14] (or graphs[11–13] or a network[15,16] or other means[17]) that cover all the useful pixels in an image. The global integral method treats the phase field as a whole since it regards two-dimensional phase unwrapping as a Poisson problem with the Neumann boundary condition.[8] For example, a least-squares (LS) method in this category attempts to minimize the distance between the esti-

W. Qiu (daniell_q@hotmail.com) and Y.-L. Kang are with the Department of Mechanics, Tianjin University, Tianjin 300072, China. Q.-H. Qin and W.-T. Li are with the Australian National University, Canberra, ACT 2600, Australia. Q.-H. Qin is with the Department of Engineering; W.-T. Li is with the Research School of Physical Sciences and Engineering.

Received 26 October 2005; revised 21 March 2006; accepted 31 March 2006; posted 4 April 2006 (Doc. ID 65595).

0003-6935/06/256551-09$15.00/0

mated and the true phase gradient by an iterative approach.[29] As for regional methods, Gierloff was the first to propose the concept of phase unwrapping by regions.[23] In his method, all the phase discontinuity-free regions are first identified and then unwrapped to eliminate the phase discontinuities at their interfaces by comparing the edge (named watershed) of each region with those of adjacent regions. In the temporal method, the phase at each pixel is regarded as a function of time, with sampling information from a series of time-lapsed fringe patterns.

Each unwrapping method has its own advantages and disadvantages. For example, the methods introduced in Refs. 13, 16, and 22 proved to be effective for processing images from synthetic interferometric aperture radar interferometry; the temporal methods are effective for electronic speckle pattern interferometry dynamic detection during production.[27] In addition, the so-called mask-cut[11] and quality-guided[12] methods are good at artificial intelligence; the minimum spanning tree method[14] is suitable for magnetic resonance imaging.

Each of the existing methods has its own limitation more or less in treating wrapped images of moiré interferometry. Generally, the regional methods seem to be more feasible than others, since they take into account phase mutations and confine them to their local regions. Most existing regional algorithm methods are claimed to be robust, but the image partition process, especially the identification of watersheds, could be difficult, fallible, or time-consuming in computation[8] with these methods. Although Huang[26] introduced transition zone into the regional partition method to supersede watersheds, general programmable partition and integral techniques are still lacking. Therefore, there is a need for new unwrapping methods that can pay equal attention to both local and global data in the processing of moiré interferometry images.

We present a new unwrapping method of regional identification, partition, and integral (RIPI) for analyzing moiré interferometry images, especially those with low quality for which both local and global data need to be taken into account equally. The principle of preorder traversal of a general tree in data structures[30,31] is first introduced to make the partition process easy and accurate, and then the idea and details of the RIPI method are given. Some examples of using the RIPI method to process images from moiré interferometry experiments are also provided, and the results are compared with those from other methods. The paper is organized as follows: in Section 2 we describe the essential principle and the mathematical description of RIPI methods; Section 3 gives a three-step algorithm for the RIPI method: partition, solution, and linear transformation; Section 4 applies the RIPI method to process images from moiré interferometry experiments and comparison is made with the other methods.

2. Essential Principle and Mathematical Description of the Regional Identification, Partition, and Integral Method

A. Phase Unwrapping

A phase image is generally acquired by processing fringe images through phase-shift or other phase-retrieval methods. A phase image is always wrapped, which does not show the real phases directly. A real phase image with continuous phase variations can be obtained only through an unwrapping process to demodulate the carrier. For example, an unwrapped phase image from moiré interferometry corresponds to the planar displacement field of the specimen.

Mathematically, the so-called wrap is to modulate the real data by a carrier with a certain frequency:

$$f_{\mathrm{WP}} = W[f_{\mathrm{TP}}] = f_{\mathrm{TP}} - \mathbf{P} \cdot \mathrm{INT}\left(\frac{f_{\mathrm{TP}} - f_{\mathrm{TP}}{}^{0}}{\mathbf{P}}\right), \qquad (1)$$

where f_{WP} and f_{TP} represent wrapped and unwrapped (or real) data, respectively; $f_{\mathrm{TP}}{}^{0}$ represents the value of f_{TP} at the origin of the spatial coordinate system; W is a wrapping function; P is the frequency of the modulating carrier; and INT represents the rounding off numbers. Obviously, unwrap means to demodulate the wrapped data and eliminate the carrier, namely,

$$f_{\mathrm{TP}} = W^{-1}(f_{\mathrm{WP}}). \qquad (2)$$

For a wrapped two-dimensional phase image, its data are the phases of all the points with the same carrier with a frequency of 2π. Thus, Eq. (1) can be transformed to

$$\phi_{\mathrm{WP}}(i, j) = \phi_{\mathrm{TP}}(i, j) - 2\pi \mathrm{INT}\left[\frac{\phi_{\mathrm{TP}}(i, j) - \phi_{\mathrm{TP}}(i_0, j_0)}{2\pi}\right]. \qquad (3)$$

An accurate or approximate solution of f_{TP} in the implicit function of Eq. (3) can be obtained by applying different algorithms based on various mathematical theories.

B. Unwrapping Method

The proposed RIPI phase unwrapping method is described as follows.

First, we simplified the two-dimensional problem into a one-dimensional case without losing its universality, as demonstrated in Fig. 1. It can be seen that the wrapping process translates all the phases into a subsection $[-\pi, \pi]$ by moving the phase integer times 2π; the unwrapping is just the inverse.

As shown in Fig. 1, the wrapped phases can be divided into some discontinuity-free regions[23] I, II, and III, which we refer to as grade regions (G regions). Inside each region, the phases (both wrapped

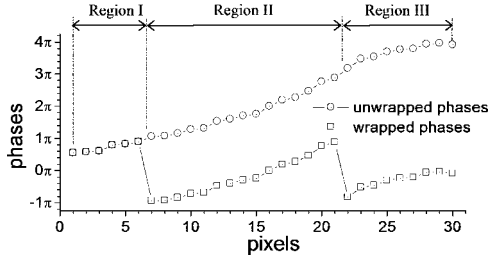

Fig. 1. One-dimensional illustration of phase unwrapping.

and unwrapped) of the points are relatively contiguous; between each region, the margins of the unwrapped phases are holistic, or rather, integer times (defined as phase grade or Grade for short) 2π. Thus, during either wrapping or unwrapping, the translations of phases are holistic. For example, in Fig. 1 the unwrapped phases of the points in region II are holistically 1 time 2π higher than those in region I; similarly, those in region III are 2 times 2π higher than those in region I. Then, unwrapped phases can be achieved by moving the wrapped phases up in region II by 1 (Grade) $\times 2\pi$, and those in region III by 2 (Grade) $\times 2\pi$.

The above principles as well as the definitions can easily be extended to two-dimensional problems. As shown in Fig. 2(a), the gray levels in the image change five times gradually from dark to white, which means all the phases of the points (pixels) in this wrapped phase image belong to five phase grades. Since the pixels with the same Grade are contiguous, the image in Fig. 2(a) can be partitioned to five G regions [Fig. 2(b)]. Ideally, the unwrapped phases can be achieved by such a discrete integral referred to as the regional integral. First, if we randomly take one G region as the relative zero G region, then the Grade of its neighboring region is $+1$ if the phases move from zero Grade to its neighbor from low to high (or -1 if from high to low), and the rest can be deduced by analogy until no G region is untouched.

We now present the mathematical descriptions of the above process. First, it is necessary to define some useful symbols. In this study, the G regions partitioned from a wrapped image are denoted as $R_{[k,k]}$, where $k \in \{1, 2, \ldots\ldots N\}$ (N is the sum of the G regions), and $[k, k]$ is defined as the serial number of $R_{[k,k]}$. Meanwhile, $\mathrm{SN}(i,j)$ is the pixel-region function that represents the serial number (SN) of the G region in which pixel (i,j) locates, namely,

$$[k,\ k] = \mathrm{SN}(i,\ j) \text{ when } (i,\ j)\ \in\ R_{[k,k]}. \tag{4}$$

In addition, $\mathbf{L}$ is the so-called grade-offset function whose independent variable is the SN of the G region, and its attributive variable is Grade. For example, $\mathbf{L}([k, k])$ is equal to the Grade of $R_{[k,k]}$, and $\mathbf{L}[\mathrm{SN}(i,j)]$ is the Grade of the G region in which a pixel (i,j) locates. Thus, in G regions, the process of unwrapping can be expressed as

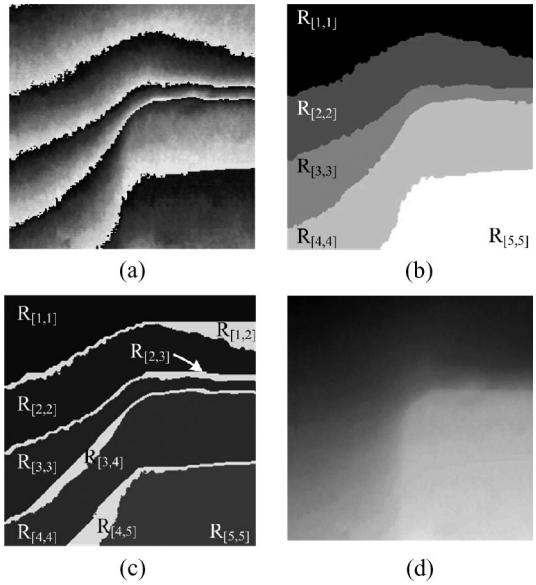

Fig. 2. Illustration of the RIPI method: (a) wrapped image, (b) G regions without T regions separated, (c) G and T regions, (d) unwrapped image.

$$\begin{aligned}\phi_{\mathrm{TP}}(i,\ j) &= W_{\mathrm{GR}}{}^{-1}[\phi_{\mathrm{WP}}(i,\ j)] \\ &= \phi_{\mathrm{WP}}(i,\ j) + 2\pi\mathbf{L}([k,\ k]) \quad (i,\ j)\ \in\ R_{[k,k]} \\ &= \phi_{\mathrm{WP}}(i,\ j) + 2\pi\mathbf{L}[\mathrm{SN}(i,\ j)].\end{aligned} \tag{5}$$

Nevertheless, as for most of the wrapped images, the formula in Eq. (5) as well as the whole procedure described above is neither applicable widely nor accurate enough, because of the contradiction between local and global characteristics. On the one hand, it is obvious from Eq. (5) that the whole process is established based on global characteristics, not on the local specifics of the image. On the other hand, local phases between any two neighboring G regions distribute discontinuously and are usually too complicated to identify their Grade. The discontinuity and complexity are both affected by several factors, such as the phase jumps induced by the modulating carrier, local acute varieties in real phases (or rather in surveying targets), the noises from all sorts of sources, and so on. Therefore, there is a significant probability to obtain inaccurate unwrapping phases near the G-region boundaries if we simply partition G regions with watersheds and apply Eq. (5).

To avoid the above problem, we separate the pixels near the boundaries from the G regions and classify them as new regions referred to as transition regions[26] [or T regions, as illustrated in Fig. 2(c)]. A T region is denoted as $R_{[k,l]}$, where $k, l \in \{1, 2\ldots\ldots N\}$ (N is the sum of the G regions) and $[k, l]$ represents the serial numbers of the two G regions next to the current T region $R\{_{k,l}\}$ are $[k, k]$ and $[l, l]$, respectively, where $k, l \in \{1, 2, \ldots\ldots N\}$ (N is the sum of the G regions). In fact, it is possible that certain T-regions could have only one or more than two neighboring G regions. As for the case of one neighboring G region, the T-region is denoted as $R_{[k,0]}$; and for the case of

more than two neighbors, it is written as $R_{[k,l,p,\ldots]}$. Even though both cases require some specific modifications during algorithmic programming, they do not affect the universality of the principle of the RIPI method and are not mentioned again in the following. In fact, the symbol $R_{[k,l]}$ can represent both the G regions and the T regions: it is a G region when $k = l$, and a T region when $k \neq l$. Analogously, almost all the functions and variables denoted in G regions can be extended to T regions, such as the pixel-region function

$$[k,\ l] = \mathrm{SN}(i,\ j) \text{ when } (i,\ j) \in R_{[k,l]}. \tag{6}$$

However, this does not apply to Grade and **L** because the phases of the pixels located in one T region belong to two phase grades with a difference of 1 Grade. In other words, if the T regions were not separated individually, these pixels would belong to two neighboring G regions.

Here, two improvements are made to unify the mathematical descriptions and then to make the algorithm feasible. First, the Grade of any T region is stipulated to be equal to the lower one of the two choices. Accordingly, $\mathbf{L}([k, l])$ could denote the grade-offset function of both the G regions and the T regions:

$$L([k,\ l]) = \min[L([k,\ k]),\ L([l,\ l])]. \tag{7}$$

At the same time, a phase-amending factor $\xi(i,j)$ is introduced to amend the unwrapping phase errors caused by the forced stipulation mentioned above. For example, if the phase of a pixel (i,j) has a certain Grade that is bigger or less than or equal to that of the T region where the pixel (i,j) locates, $\xi(i,j)$ is set to $+1$, -1, or 0, respectively. Thus, in the T regions, the unwrapping process can be conducted using

$$\begin{aligned}\phi_{\mathrm{TP}}(i,\ j) &= W_{\mathrm{TR}}{}^{-1}[\phi_{\mathrm{WP}}(i,\ j)] \\ &= \phi_{\mathrm{WP}}(i,\ j) + 2\pi\mathbf{L}[\mathrm{SN}(i,\ j)] + 2\pi\xi(i,\ j).\end{aligned} \tag{8}$$

By stipulating $\xi(i,j) = 0$, where $(i,j) \in R_{[k,k]}$, it is rational to combine Eq. (5) with Eq. (8) to obtain

$$\begin{aligned}\phi_{\mathrm{TP}}(i,\ j) &= W^{-1}[\phi_{\mathrm{WP}}(i,\ j)] \\ &= \phi_{\mathrm{WP}}(i,\ j) + 2\pi\mathbf{L}[\mathrm{SN}(i,\ j)] + 2\pi\xi(i,\ j).\end{aligned} \tag{9}$$

Therefore, if $\mathbf{L}[\mathrm{SN}(i,j)]$ and $\xi(i,j)$ of each pixel are available, the unwrapping can be achieved by use of Eq. (9). However, the following two complementary factors need to be considered. First, for the G regions, k in the serial number $[k, k]$ is just a random number to distinguish one G region from the others; and for the T regions, either k or l is not discretionary, but depends completely on the serial number of the nearby G regions. Second, $\mathbf{L}[k, k]$ is not absolute, but is relative to the selection of the G region of 0 Grade; however, the Grade difference between any two G regions is absolute. Therefore, as shown in Fig. 2(c), if we select $R_{[l,l]}$ as the zero Grade G region (namely, $\mathbf{L}([1, 1]) = 0$), we have $\mathbf{L}([2, 2]) = 1$ and $\mathbf{L}([2, 2]) - \mathbf{L}([1, 1]) = 1$; or if selecting $R_{[2,2]}$ as the zero Grade G region ($\mathbf{L}([2, 2]) = 0$), we have $\mathbf{L}([1, 1]) = -1$ and $\mathbf{L}([2, 2]) - \mathbf{L}([1, 1]) = 1$. Hence, the above two complements ensure that the computer program is flexible and the unwrapping result is unique.

In summary, the main principle of the RIPI unwrapping method is to identify the Grade of each pixel (i, j), to partition the G and T regions in the wrapped phase image, then obtain the solutions of $\mathbf{L}[\mathrm{SN}(i, j)]$ and $\xi(i, j)$ by means of a regional integral, and finally to obtain the unwrapped phase f_{TP}.

3. Algorithm and Programming

The algorithm of the RIPI phase unwrapping method comprises three mean steps: partition, solution, and linear transformation.

A. Partition

Partition, or region partition, is the first and most important step of the RIPI method because it is the basis of this unwrapping method. In other words, partition is the kernel that makes the RIPI method differ from other unwrapping methods.

1. Categorization

We divide the partition into three substeps. The first is categorization, which classifies all pixels into either G-region or T-region groups. As for a wrapped phase image, we can eyeball where to locate the G regions and the T-regions, but this is a manual and rough classification. We used a categorical technique that is a combination of threshold function and a preset transitional phase to pick out the pixels of the T-regions from the image.

The threshold function,[26] with a window of $(2N + 1) \times (2N + 1)$ pixels^2, is written as

$$\sum_{m=-N}^{N}\sum_{n=-N}^{N} \mathrm{INT}\left|\frac{\phi(i,\ j) - \phi(i+m,\ j+n)}{\pi}\right| > \mathrm{THR}, \tag{10}$$

where THR is the threshold whose theoretical value is

$$\mathrm{THR}_{\mathrm{theory}} = (N^2 - 1)/2. \tag{11}$$

If we set $N = 5$, then $\mathrm{THR}_{\mathrm{thoery}} = 12$ from Eq. (11). During practical image processing, such a high THR value always, however, leads to a break within a T region and to the misconnection of different G regions that are due to the existence of noise and phase defects. To avoid this, the practical THR value is usually determined by

$$\mathrm{THR}_{\mathrm{practice}} = (N^2 - 1)/M \quad (M > 2). \tag{12}$$

As an empirical value, here we use $M = 3$, then $\mathrm{THR}_{\mathrm{practice}} = 8$.

In addition to the above consideration, a preset

transitional phase (e.g., $5\pi/6$) is also used for the categorization step. Such a pixel will be put into the T region as long as the following two conditions are met: (1) the absolute value of the pixel phase surpasses the preset transitional phase and (2) the pixel is located at the neighbor of any of the T regions, which have already been identified by the threshold function. After processing, the image is divided into different G and T regions. Each G region is isolated from another by a T region and each T region by G regions. In a G region all the pixels have the same Grade, but the pixels having the same Grade may not be in the same G region.

2. Arrangement

The second substep of partition is the arrangement, which is to identify the pixels located in the same region and then assign a SN to this region. To implement this substep, the principle of preorder traversal of a general tree in the data structures[30,31] is introduced first. Figure 3(a) is an example of a general tree, in which T, L, M, R, A, B, C, D, E, and F are nodes. T is the root of this tree and the parent of L, M, and R. In other words, L, M, and R are siblings, and they are all the children of T. The relationships between the nodes in other tree branches are similar to those between L, M, R, and T mentioned above. In detail, L is the parent of siblings A, B, C; M is the parent of D; R is the parent of siblings E and F. In addition, a rectangle surrounds the subtree having L as its root. A preorder traversal of a general tree first visits the root of the tree and then performs a one by one preorder traversal of each subtree. As for the tree in Fig. 3(a), a preorder traversal visits the nodes in the following order: $T \rightarrow L \rightarrow A \rightarrow B \rightarrow C \rightarrow M \rightarrow D \rightarrow R \rightarrow E \rightarrow F$. The substep of the RIPI arrangement based on the principle of preorder traversal is illustrated by the flow chart shown in Fig. 3(b) and is described as follows.

(A) Start from a virgin pixel (as the root), which has not been assigned to any region (after a pixel is assigned to a region, it is no longer a virgin); open a new region (a new tree), assign a serial number to it and regard it as the current region; then go to step (B).

(B) Assign the current pixel to the current region and examine whether it has any virgin neighbors (as its children, not its siblings) that belong to the same category (G region or T region). If it has children, regard these children as siblings, select the first one from the left (of this branch) as the current pixel, and repeat (B); otherwise, go to step (C).

(C) Examine whether the current pixel has virgin sibling pixels. If it has, select the first one from the left as the current pixel, and go to (B); if it does not have virgin sibling pixels, but its parent is not the root, use the parent as the current pixel and repeat (C); otherwise, go to (D).

(D) End this region arrangement and begin a new one.

Since it is one's own discretion which serial number should be assigned to any G region but not to any T region, we assign serial numbers to all G regions first and then to T regions. When we define a new T region, its serial number is set according to the G regions next to it. When no pixel is virgin, the image is partitioned into many G and T regions with their own serial numbers.

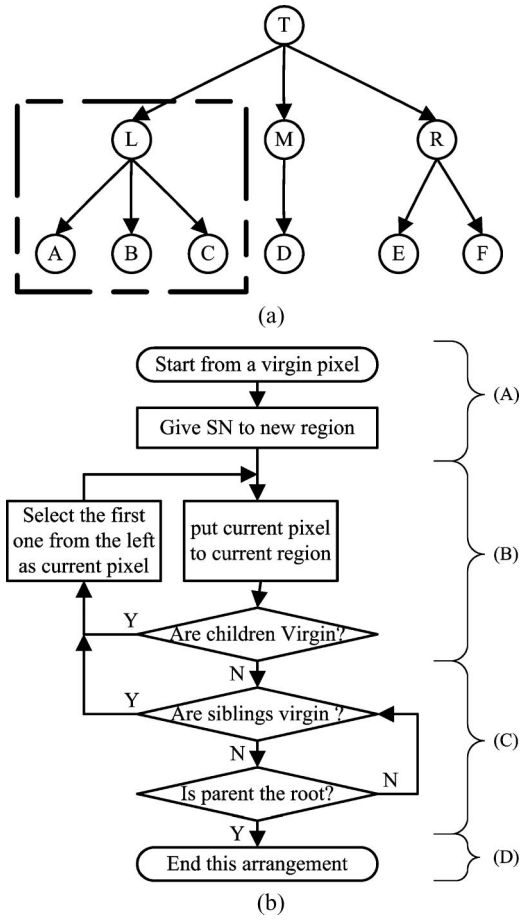

Fig. 3. (a) Example of a general tree. (b) Flow chart of the substep arrangement based on the principle of preorder traversal of a general tree.

3. Rearrangement

After finishing the above arrangement, one would know that the total number of regions is always much larger than what the image should have. Visually, there are quite a few islands among some big regions. These islands, which we refer to as pseudoregions, are the small regions induced by acute gradation of local information that includes both valid phases and noises. In our research, the threshold of the minimal pixel number in a region is used to eliminate the pseudoregions by incorporating them into their surrounding regions. Then, by repeating the arrangement substep (maybe several times), the image phase can be partitioned into different G and T regions correctly.

B. Solution

This step is used to solve the grade-offset function $\mathbf{L}[\mathrm{SN}(i,j)]$ and then to get the phase-amending factor

$\xi(i, j)$ of all pixels. As for the grade-offset function, it is not necessary to solve $\mathbf{L}[\mathrm{SN}(i, j)]$ for every pixel (i, j). According to Eq. (6) obtaining only the solutions of $\mathbf{L}[(k, l)]$ is sufficient. Here we introduce the following two methods for a regional integral to obtain the solutions of $\mathbf{L}[(k, l)]$.

1. G Regions All Path

We integrate the grades of all regions along preset paths that pass through all the G regions, named the G regions all path. In fact, there must be paths, such as those that go over the image pixel by pixel and row by row. Thus, so as not to lose its generality, we take one path as the example.

Before a regional integral, a status factor $\eta([k, k], [k, l])$ is defined as follows. When the path travels in $R_{[k,k]}$ and approaches the boundary of $R_{[k,k]}$ and $R_{[k,l]}$, if the phase mean of the pixels that the path will currently pass by before leaving $R_{[k,k]}$ is less than 0, we have $\eta([k, k],[k, l]) = -1$, meaning $\mathbf{L}([k, k]) - 1 = \mathbf{L}([k, l])$; or if it is larger than 0, we have $\eta([k, k], [k, l]) = 0$, meaning that $\mathbf{L}([k, k]) = \mathbf{L}([k, l])$. Thus, if the path is confirmed, the status factors $\eta([k, k], [k, l])$ at any G- or T-region boundary along the path can be obtained. The regional integral by use of the G-regions-all-path method is conducted with the following processes.

(A) Set the first G region to be passed by the selected path as the relative zero grade region.

(B) When the path leaves a G region (assumed as $R_{[k,k]}$), passes a T region (assumed as $R_{[k,l]}$), and enters $R_{[l,l]}$, $\mathbf{L}([l, l])$ can be written as

$$L([l,\ l]) = L([k,\ k]) - \eta([k,\ k],\ [k,\ l]) + \eta([k,\ l],\ [l,\ l]), \tag{13}$$

where $\mathbf{L}([k, k])$ is known since the path has left $R_{[k,k]}$.

(C) After every $\mathbf{L}([k, k]\ k \in \{1, 2, \ldots\ldots N\}$ (N is the sum of the G regions) is obtained, the solutions of the $\mathbf{L}([k, l])$ can be obtained by applying Eq. (7), and thus the Grade of each region is obtained.

In fact, there are obvious differences between this regional integral and the path-following integral used in local methods,[4,9–17] which can be generally expressed as

$$\phi_{\mathrm{TP}}[P(i)] = \int_{S_k{}^0}^{i} [1 - \alpha(i)]\mathrm{d}\phi_{\mathrm{WP}}[P(i)], \tag{14}$$

where

$$\alpha(i) = 0 \text{ when } \mathrm{d}\phi_{\mathrm{WP}}[P(i)] \neq 2\pi,$$
$$\alpha(i) = 1 \text{ when } \mathrm{d}\phi_{\mathrm{WP}}[P(i)] = 2\pi.$$

First, the former (regional integral) evaluates Grade region by region, but the latter (path integral) evaluates unwrapping phases pixel by pixel in the image. More importantly, the path in the latter plays a decisive role in the effect of unwrapping results: a proper choice of the path will lead to a better effect, and a bad choice will cause a worse result. Solutions sometimes cannot even be found by use of the path-following unwrapping methods. In fact, numerous unwrapping algorithms based on the path-following integral principle have been developed to explore the optimal integral path. The path of our regional integral method only needs to go through all G regions, and the unwrapping results are identical even if integrating through different paths. In short, the RIPI method is independent of path selection.

2. Region-Relation Tree

Another method for performing the regional integral is with a region-relation tree. With this method the Grades of the regions are integrated through building a region-relation tree. In fact, after partition, one of the outputs is a data chain [named a serial number (SN) chain] storing the SNs of all the G regions and T regions. But this chain does not include the phase relation between any two regions. Here we present a data tree called the region-relation tree to establish the relations among all the regions. In the region-relation tree, all the nodes are looked at as G regions, and T is omitted. The regional integral processing based on the region-relation tree is carried out according to the following steps:

(A) Build the region-relation tree of the image in preorder.

(1) Select a G region randomly as the root node and regard it as the relative zero Grade region. Scan the SN chain to find the neighboring G regions of the root and then set them as children nodes of the root.

(2) When a G region has been incorporated into the tree, scan the SN chain to determine its neighboring G regions that have not yet been included in the tree, then fix these G regions in the tree as its children nodes, and then repeat.

(3) If a branch of the tree reaches its end, go to the nearest siblings or parent's siblings or grandparent's siblings (and so on) that is not at the end of a branch, and then repeat (2).

When all branches have been gone through, in other words, when all the G regions have been incorporated into the tree, the region-relation tree has been built.

(B) Evaluate every $\mathbf{L}([k, l])$ where η is the status factor defined above.

(1) Visit all the nodes in the region-relation tree in preorder.

(2) At any node $[l, l]$, evaluate $\mathbf{L}[l, l]$ by use of Eq. (15) beginning with the reference path from a random pixel in $R_{[k,k]}$, passing a random pixel in $R_{[k,l]}$, and then terminating at a random pixel in $R_{[l,l]}$:

$$L([k,\ l]) = L([k,\ k]) + \eta([k,\ l],\ [l,\ l])$$

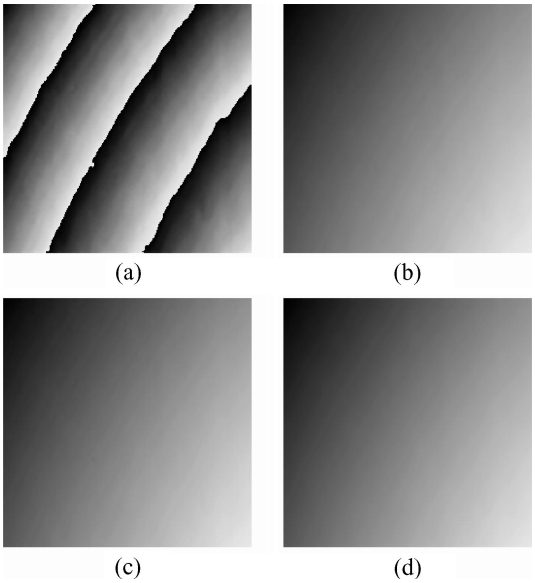

Fig. 4. (a) Wrapped phase image of high quality, (b) unwrapped image obtained with the classical method, (c) unwrapped image obtained with the Kadono method, (d) unwrapping obtained with the RIPI method.

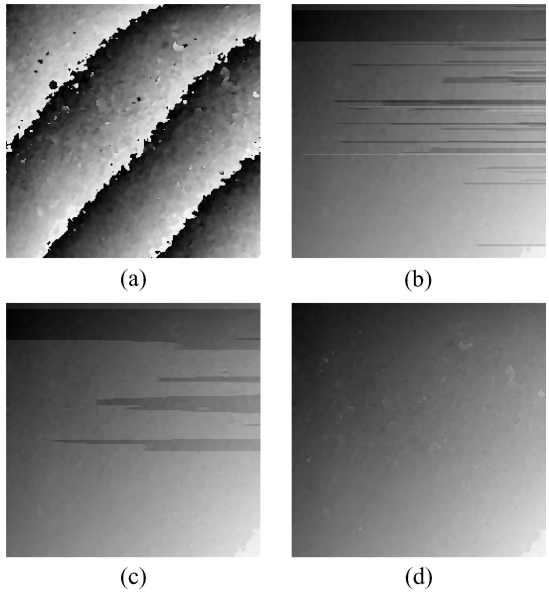

Fig. 5. (a) Wrapped phase image of low quality, (b) unwrapped image obtained with the classical method, (c) unwrapped image obtained with the Kadono method, (d) unwrapping obtained with the RIPI method.

$$L([l,\ l]) = L([k,\ k]) - \eta([k,\ k],\ [k,\ l]) + \eta([k,\ l],\ [l,\ l]). \quad (15)$$

(3) If $\mathbf{L}([k, l])$ cannot be obtained using Eq. (15) (generally this T region has only one neighboring G region), it can be evaluated by

$$L([k,\ l]) = L([k,\ k]) - \eta([k,\ k],\ [k,\ l]) - 1, \quad (16)$$

with the reference path started from a random pixel in $R_{[k,k]}$, terminated at a random pixel in $R_{[k,l]}$. The Grades of all the regions have thus been obtained.

If we compare the above two methods, it can be seen that they are based on the same principle, the regional integral, but are implemented in different ways. Actually, the first method, the G regions all path, is easier for programming, whereas the second method, region-relation tree, is more precise for mathematical logic.

3. Phase-Amending Factor

For the phase-amending factor $\xi(i, j)$, we use $\xi(i, j) = 1$ if the wrapped phase at (i, j) is >0; otherwise $\xi(i, j) = 0$ if the wrapped phase is <0.

C. Linear Transformation

We can now substitute $\mathbf{L}[\mathrm{SN}(i, j)]$ and $\xi(i, j)$ into Eq. (9) at each pixel (i, j), and then linearly transforms all the $\phi_{\mathrm{TP}}(i, j)$ to the phase region of $[-\pi, \pi]$, so that the phase unwrapping of the wrapped image by means of the RIPI method is finished. We implemented RIPI programming by using Visual C++ 6.0.

4. Applications of the Regional Identification, Partition, and Integral Unwrapping Method

Here we present some examples of applying the RIPI unwrapping method to process images obtained from moiré interferometry experiments.

A. Comparison of Unwrapping Methods

To demonstrate the advantages of the RIPI over other unwrapping methods, we applied the RIPI and two other existing methods to process some wrapped images with different qualities. A high-quality image is shown in Fig. 4(a), a low-quality image is shown in Fig. 5(a), and an ultralow-quality image is shown in Fig. 6(a). Figures 4(b), 5(b), and 6(b) show the unwrapped results that were obtained with the classical method outlined in Ref. 5. Figures 4(c), 5(c), and 6(c) represent the results generated by use of the Kadono method reported in Ref. 9. Figures 4(d), 5(d), and 6(d) illustrate the results obtained with the RIPI method.

Figure 4 shows that all the applied unwrapping methods can generate good results if the original wrapped image is of high quality. If the wrapped phase image is of low quality, many line defects are generated in the unwrapped image by use of the classical method as shown in Fig. 5(b). The results are not obviously improved by application of the Kadono method because it cannot deal with a significant amount of noise speckles and phase singularities. However, the RIPI technique confines the effects of noise and singularity to their local areas separately, so line defects are completely avoided. As for a phase image of ultralow quality such as that in Fig. 6(a), only the RIPI method can lead to a satisfactory outcome, whereas the other two methods create many line defects. Therefore, the RIPI method has a dis-

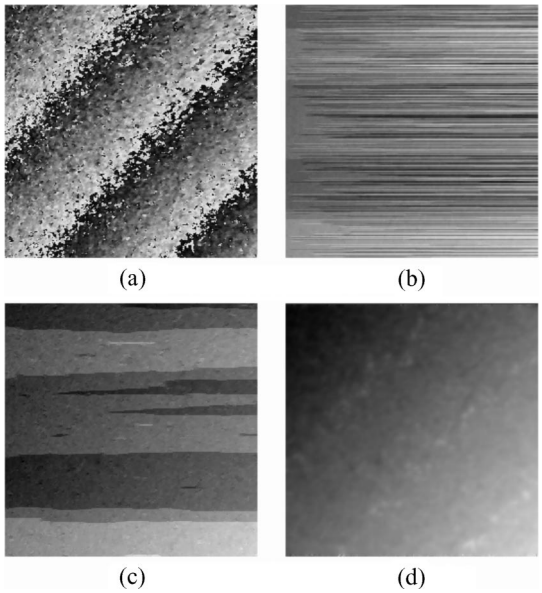

Fig. 6. (a) Wrapped phase image of ultralow quality, (b) unwrapped image obtained with the classical method, (c) unwrapped image obtained with the Kadono method, (d) unwrapping obtained with the RIPI method.

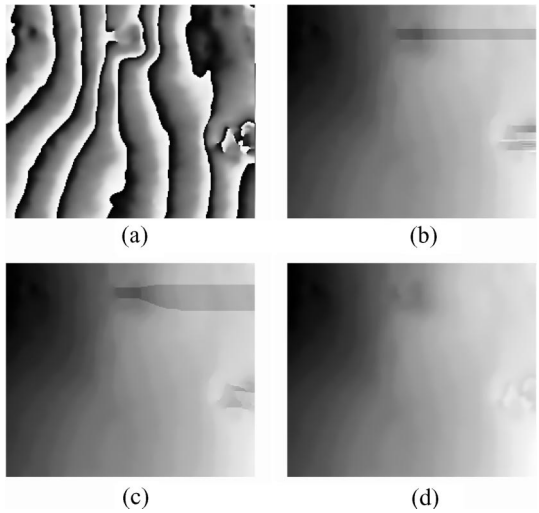

Fig. 7. (a) Wrapped phase image of moiré interferometry on a multilayer piezoelectric structure, (b) unwrapped image obtained with the classical method, (c) unwrapped image obtained with the Kadono method, (d) unwrapping obtained with the RIPI method.

tinct advantage over others in processing low-quality and even ultralow-quality images.

B. Experimental Example

We have also successfully applied the RIPI technique to process our experimental results on piezoelectric material analyses. The aim of the experiment is to study the stress and geometric configuration of a multilayer piezoelectric displacement actuator.[3] Because the piezoelectric part of an apparatus is always very small (hundreds of micrometers or less thick) and a high voltage is applied to it during operation, it is thus extremely difficult to conduct mechanical experiments to obtain information about the stress and deformation of the material. Moiré interferometry is almost the best method to measure the local surface deformation of piezoelectric materials, but the images obtained are usually of low quality. Figure 7(a) shows that there are two large defects in the upper center and lower right parts of the phase image. The unwrapped image in Fig. 7(d) is much better than the images in Figs. 7(b) and 7(c) that were obtained by use of the classical and the Kadono methods.

C. Execution Time and Memory Usage

All the images discussed in this paper were processed with a 1.5 GHz Pentium IV CPU computer with 256 Mbytes DDR266 RAM, and a WindowsXP operating system. The execution time required for a 256×256 pixels^2 image is less than 1 s, and the peak amount of memory used was less than 12 Mbytes; for an image with 512×512 pixels^2, the time was approximately 2 s and the amount of memory used was less than 60 Mbytes. Therefore it is not time-consuming or memory consuming when the RIPI method is used to process moiré interferometry images. In addition, the images obtained from moiré interferometry experiments are not very large (generally less than 1M pixels), and it is not necessary to process images in real time during a moiré interferometry measurement. Hence, the RIPI method should have significant potential use in practical applications.

5. Conclusion

We have presented a new unwrapping method based on the ideas of regional identification, partitioning, and integral. The basic concept, mathematical description, and algorithm of the RIPI method have been presented. As far as we know, this is the first time that the principle of preorder traversal of a general tree has been introduced into an unwrapping processing, which makes the partition process easy to implement and provides accurate results. The methods for a regional integral were also introduced to solve the phase grade. Moreover, examples of application of the RIPI method to process images of moiré interferometry experiments have been provided. We have demonstrated that the RIPI method is superior over other existing methods for processing low-quality images of moiré interferometry.

The authors acknowledge the financial support of the National Natural Science Foundation of China (SN 10232030) and the 2005 Endeavour Australia Cheung Kong Award.

References

1. D. Post, B. Han, and P. Ifju, *High Sensitivity Moiré Experimental Analysis for Mechanics and Materials* (Springer-Verlag, 1994).
2. W. Lu, D. N. Fang, and K. C. Hwang, "A constitutive theory for ferroelectric ceramics," Key Eng. Mater. **145,** 983–988 (1998).
3. W. Qiu, Y. Kang, Q. Sun, Q. Qin, and Y. Lin, "Stress analysis and geometrical configuration selection for multilayer piezo-

electric displacement actuator," Acta Mech. Solida Sin. **17,** 323–329 (2004).
4. K. Itoh, "Analysis of the phase unwrapping algorithm," Appl. Opt. **21,** 2470 (1982).
5. D. J. Bone, "Fourier fringe analysis: the two-dimensional phase unwrapping problem," Appl. Opt. **30,** 3627–3632 (1991).
6. M. Kujawinska, "Automated in-plane moiré techniques and grating interferometry," in *Optical Methods in Experimental Solid Mechanics,* K.-H. Laermann, ed. (Springer-Verlag, 2000), pp. 123–195.
7. D. C. Ghiglia and M. D. Pritt, *Two-Dimensional Phase Unwrapping: Theory, Algorithms, and Software* (Wiley, 1998).
8. A. Baldi, F. Bertolino, and F. Ginesu, "On the performance of some unwrapping algorithms," Opt. Lasers Eng. **37,** 313–330 (2002).
9. H. Kadono, H. Takei, and S. Toyooka, "A noise-immune method of phase unwrapping in speckle interferometry," Opt. Lasers Eng. **26,** 151–164 (1997).
10. R. M. Goldstein, H. A. Zebker, and C. L. Werner, "Satellite radar interferometry: two dimensional phase unwrapping," Radio Sci. **23,** 713–720 (1988).
11. A. Asundi and Z. Wensen, "Fast phase-unwrapping algorithm based on a gray-scale mask and flood fill," Appl. Opt. **37,** 5416–5420 (1998).
12. C. Quan, C. J. Tay, L. Chen, and Y. Fu, "Spatial-fringe-modulation-based quality map for phase unwrapping," Appl. Opt. **42,** 7060–7065 (2003).
13. T. J. Flynn, "Two-dimensional phase unwrapping with minimum weighted discontinuity," J. Opt. Soc. Am. A **14,** 2692–2701 (1997).
14. N. H. Ching, D. Rosenfeld, and M. Braun, "Two-dimensional phase unwrapping using a minimum spanning tree algorithm," IEEE Trans. Image Process. **1,** 355–365 (1992).
15. M. Costantini, "A novel phase unwrapping method based on network programming," IEEE Trans. Geosci. Remote Sens. **36,** 813–821 (1998).
16. M. Hubig, S. Suchandt, and N. Adam, "Equivalence of cost generators for minimum cost flow phase unwrapping," J. Opt. Soc. Am. A **19,** 64–70 (2002).
17. D. C. Ghiglia, G. A. Mastin, and L. A. Romero, "Cellular-automata method for phase unwrapping," J. Opt. Soc. Am. A **4,** 267–280 (1987).
18. M. D. Pritt and J. S. Shipman, "Least-squares two-dimensional phase unwrapping using FFT's," Trans. Geosci. Remote Sens. **32,** 706–708 (1994).
19. D. Kerr, G. H. Kaufmann, and G. E. Galizzi, "Unwrapping of interferometric phase-fringe maps by the discrete cosine transform," Appl. Opt. **35,** 810–816 (1996).
20. G. H. Kaufmann, G. E. Galizzi, and P. D. Ruiz, "Evaluation of a preconditioned conjugate-gradient algorithm for weighted least-squares unwrapping of digital speckle-pattern interferometry phase maps," Appl. Opt. **37,** 3076–3084 (1998).
21. M. D. Pritt, "Phase unwrapping by means of multigrid techniques for interferometric SAR," IEEE Trans. Geosci. Remote Sens. **34,** 728–738 (1996).
22. D. C. Ghiglia and L. A. Romero, "Minimum L^p-norm two-dimensional phase unwrapping," J. Opt. Soc. Am. A **13,** 1999–2013 (1996).
23. J. J. Gierloff, "Phase unwrapping by regions," in *Current Developments in Optical Engineering II,* R. E. Fischer and W. J. Smith, eds., Proc. SPIE **818,** 2–9 (1987).
24. Q. Lin, J. F. Vesecky, and H. A. Zebker, "Phase unwrapping through fringe-line detection in synthetic aperture radar interferometry," Appl. Opt. **33,** 201–208 (1994).
25. P. Soille, "Morphological phase unwrapping," Opt. Lasers Eng. **32,** 339–352 (2000).
26. M. J. Huang, "A quasi-one-frame phase-unwrapping algorithm through zone-switching and zone-shifting hybrid implementation," Opt. Commun. **210,** 187–200 (2002).
27. J. M. Huntley and H. Saldner, "Temporal phase-unwrapping algorithm for automated interferogram analysis," Appl. Opt. **32,** 3047–3052 (1993).
28. H. O. Saldner and J. M. Huntley, "Temporal phase unwrapping: application to surface profiling of discontinuous objects," Appl. Opt. **36,** 2770–1275 (1997).
29. M. D. Pritt, "Comparison of path-following and least-squares phase unwrapping algorithms," in *Proceedings of the International Geoscience and Remote Sensing Society* (Institute of Electrical and Electronics Engineers, 1997), pp. 872–874.
30. A. V. Aho, *Data Structures and Algorithms* (Addison-Wesley, 1985).
31. C. A. Shaffer, *A Practical Introduction to Data Structures and Algorithm Analysis,* 2nd ed. (Prentice–Hall, 2001).